Planar Surface-Wave Sources and Metallic Grating Lenses for Controlled Guided-Wave Propagation

Symon K. Podilchak, *Member, IEEE*, Al P. Freundorfer, *Senior Member, IEEE*, and Yahia M. M. Antar, *Fellow, IEEE*

***Abstract*—Guided surface-waves (SWs) on planar substrates are generally an adverse effect that can degrade the performance of monolithic integrated circuits and antenna arrays. However, with appropriate boundary conditions, such SWs can be harnessed as an efficient means of power transport achieving bound propagation along a dielectric slab. Furthermore, by the addition of planar metallic grating configurations an effective dielectric constant can be achieved, refracting cylindrical SWs transmitted from a central surface-wave launcher (SWL) source. Specifically, two metallic grating lenses are investigated for millimeter-wave frequencies of operation, offering either the convergence or divergence of bound SWs. In addition, design concepts are extended to a novel planar coupler. These metallic grating lenses and directive SWL sources can be useful for new quasi-optical millimeter-wave circuits and planar leaky-wave antennas.**

***Index Terms*—Lens, surface-wave (SW), surface-wave launcher (SWL).**

I. Introduction

THE CONCEPT OF lensing at microwave and millimeter-wave frequencies has been seen in many antenna feeding networks and power distribution systems [1], [2]. In these designs dielectric lens are generally used to control field distributions propagating from a central source; i.e., two different materials are used to achieve refraction. In [2], a dielectric lens (or air gap) within a grounded dielectric slab (GDS) was investigated for cylindrical TM surface-wave (SW) focusing from a network of surface-wave launchers (SWLs). That proposed power combiner was novel, but practical fabrication of such a design would be difficult since a finely shaped dielectric lens would be required within a main GDS.

In an effort to ease fabrication in such complex systems new planar lenses are proposed. Specifically, by utilizing printed metallic grating configurations (placed on top of a GDS, as illustrated in Fig. 1) control of guided SWs is possible [3]. The investigated lenses (Fig. 2) offer the divergence and convergence of cylindrical SWs. Printed lens sources are realized by directive SWL elements [4] (which have been previously used in the design of planar leaky-wave antennas [5], [6]). In the presented lens configurations (for bound and guided-wave propagation) the radial electric field of the excited TM_0 SW mode couples to the gratings and the majority of the electric field near the strips is contained within the slab, suggesting the excitation of a hybrid microstrip mode [7], [8].

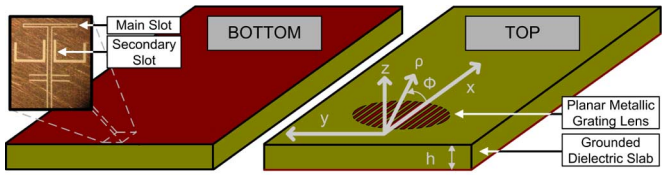

Fig. 1. (a) SW source in the ground plane and (b) planar grating lens on top of the GDS. Origin defined on the air-dielectric interface at the center of the main slot of the directive SWL. Note: Illustration not to scale.

In addition, such grating lenses and SW sources [4] can be utilized in the design of quasi-optical millimeter-wave circuit systems [1], [2] and novel planar antennas. Specifically, if a SWL array (as presented in [6]) is utilized as shown in Fig. 3, new types of planar circuits can be realized. For instance, by changing the relative phase difference between two transmit SWL array elements ($\delta = \Phi_2 - \Phi_1$) propagating SWs can be routed to specific receiver SWLs. A grating lens can also be used for improved directivity and isolation. Secondary circuits, such as amplifiers and or antennas can be connected to the receiver SWLs for increased diversity and functionality. Furthermore, such grating lenses can also be used in conjunction with planar antennas for beam control in the far-field.

II. SW Sources for Bound Propagation

The planar sources for directive SW propagation are realized by slots in the ground plane of a dielectric slab and are fed by coplanar waveguide transmission lines [4]–[6]. The frequency of operation and slab characteristics ($\epsilon_r = 10.2, h = 1.27$ mm, $\tan\delta = 0.0023$) defines this bound SW propagation along the guiding surface.

A. Field Distributions Generated by the SW Source

The magnitude of the E_z field distribution along the guiding surface was measured by placing the SWL at the edge of a large GDS and results are compared to simulated values (Fig. 4). The evanescent TM SW field distributions were sampled above the guiding surface as further described in Fig. 5. Results are also compared to a typical cylindrical-wave ($\approx E_0/\rho^{(1/2)}$) with reasonable agreement. Minor deviations are observed and are likely a result of substrate surface roughness, reflections from the edge of finite substrate, and dielectric thickness and probe height variations along the guiding surface.

Physically, the SWL couples energy into the dominant TM_0 SW mode of the slab and thus a useful comparison can be between the rate of TM field strength roll off away from the

Manuscript received December 26, 2008. First published January 27, 2009; current version published May 20, 2009.

S. K. Podilchak and A. P. Freundorfer are with the Department of Electrical and Computer Engineering, Queen's University, Kingston, ON K7L 3N6, Canada.

Y. M. M. Antar is with the Electrical Engineering Department, Royal Military College of Canada, Kingston, ON K7K 7B4, Canada.

Color versions of one or more of the figures in this letter are available online at http://ieeexplore.ieee.org.

Digital Object Identifier 10.1109/LAWP.2009.2013488

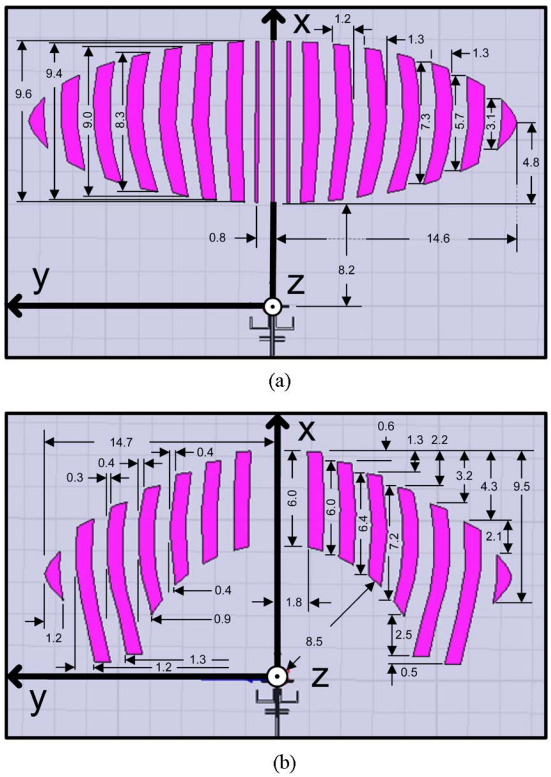

Fig. 2. Planar lens configurations (dimensions in mm) for (a) diverging and (b) converging of SWs. Periodicity for the grating: 0.8 mm. (a) Width of three inner strips 0.15 mm, remaining strips 0.9 mm. (b) Strip width 0.9 mm.

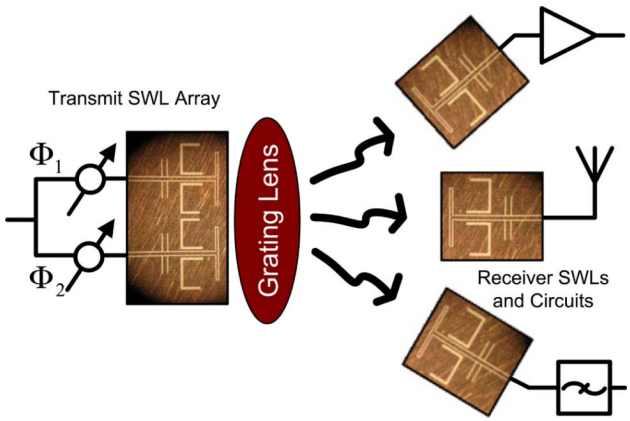

Fig. 3. Application to planar millimeter-wave circuit systems. An array of transmit SWLs can steer guided-waves to specific receiver SWLs by changing the relative phase difference between elements ($\delta = \Phi_2 - \Phi_1$). Secondary circuits can be amplifiers, antennas, filters and/or other passive and active elements. A grating lens can also be used for performance improvements.

source as shown in Fig. 4. For instance for $x \in [+10, +20]$ mm, $\Delta|E_z| = -0.30[-0.35]\langle -0.33\rangle$ dB/mm V/m for the analytical [simulated] ⟨measured⟩ field distribution. In addition, TE SWs can also exist on the GDS since operation is above the cutoff frequency of the TE_1 SW mode of the slab (19.47 GHz).

The full $|E_z(x, y)|$ field distribution can also be analyzed. Fig. 6(a) shows the forward directed cylindrical-wave gradually spreading out along the guiding surface; $|E_z| \geq 750$ V/m in the confined 1 520 mm^2 region (defined by $x \in [0, +40]$ mm and $y \in [-19, +19]$ mm). In addition, the folded secondary slots

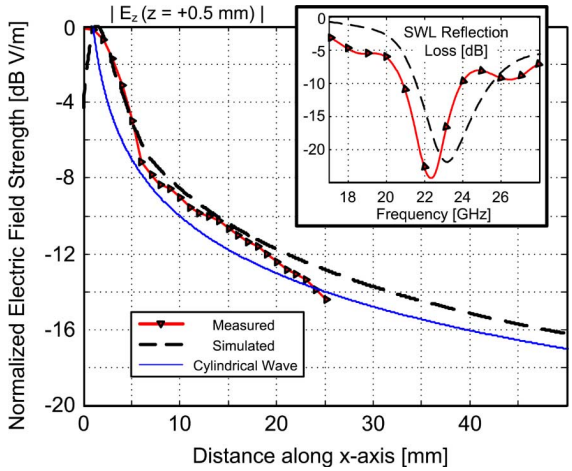

Fig. 4. Measured [simulated] values were obtained at 23 [24] GHz by observing the field distributions above the guiding surface. Reflection loss values are also shown for the planar directive SWL.

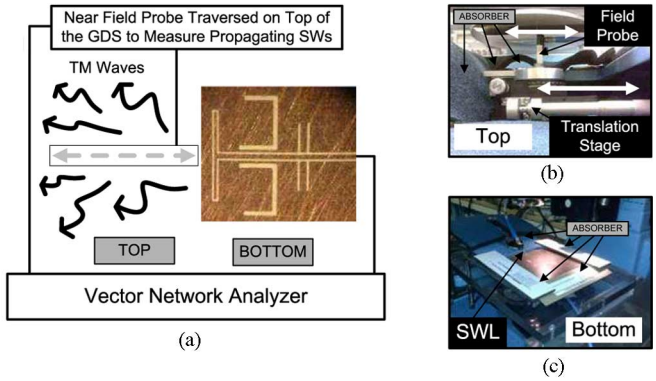

Fig. 5. Technique to observe the evanescent TM SW field distribution 0.5 mm above the guiding surface (an analogous procedure, using Ansoft's HFSS near field analysis, was utilized for simulations). (a) The system was connected to a VNA and field strength values were collected using a near-field probe in 1 mm increments for $x = [0, 25]$ mm. (b) The probe was mounted on a linear translation stage and field values were measured on top of the GDS. (c) The SWL was excited and absorber was used to minimize reflections (bottom).

increase forward directivity while exciting TE SWs in the $\pm\hat{y}$ directions as shown in the $|E_\phi(x, y)|$ field distribution, specifically $|E_\phi| \leq 500$ V/m for $y = \pm 19$ mm.

B. *Performance of the SWL*

Measured and simulated reflection losses are shown in the inset of Fig. 4. A slight frequency shift is shown; i.e., minimum reflection loss is observed at 22.2 [23.6] GHz in the measurements [simulations]. These slight deviations may be attributed to slab height and dielectric variations, fabrication tolerances, and slot modeling difficulties due to microfabrication.

Additional investigations may also be required to illustrate the bound nature of the excited SWs and, thus, describe further their performance and general operation. For instance, the negligible parasitic far-field radiation from a single SWL element and the minimal insertion loss between two sources can further illustrate this bound and guided-wave propagation:

1) Parasitic Radiation Into the Far-Field: The majority of the excited SW power is bound to the slab and not radiated [4]. Measured gain values (<1.75 dB) are observed at 22.25 GHz (in

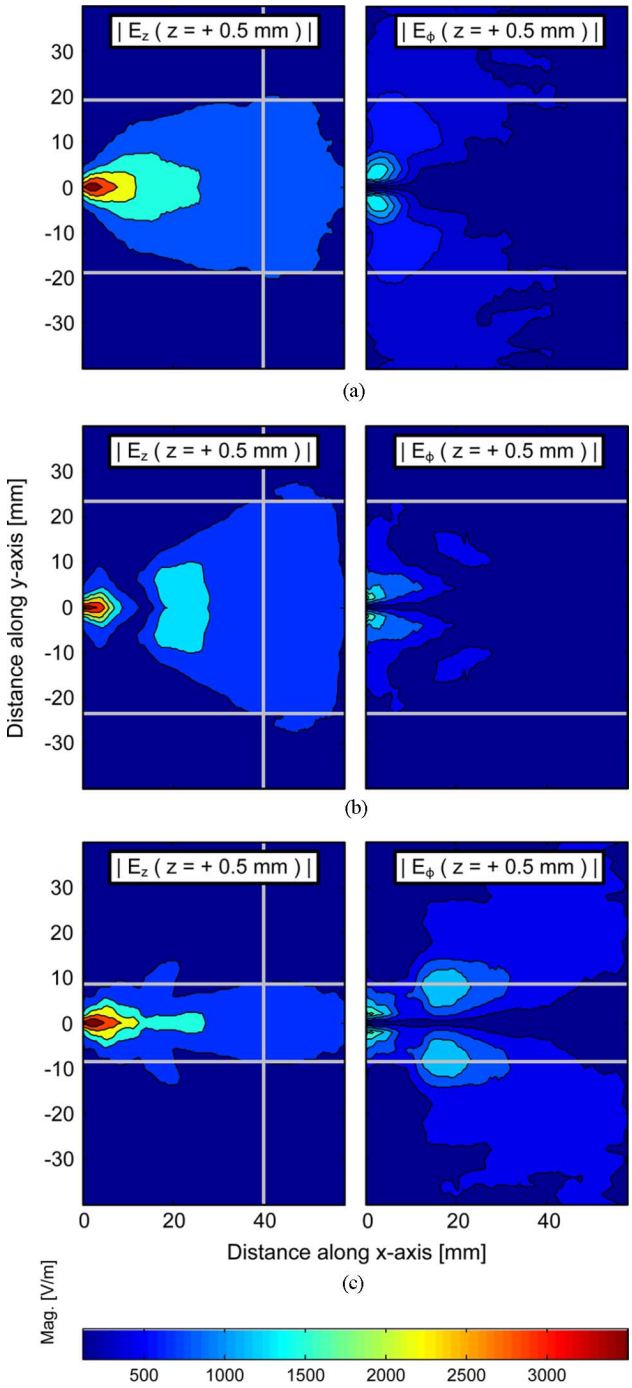

Fig. 6. Simulated TM and TE field distributions, $|E_z|$ and $|E_\phi|$, at 24 GHz: (a) single SWL. (b) Diverging. (c) Converging lenses.

the upper half region, $z > 0$) as shown in Fig. 7(a), with a reasonable agreement to the simulated values at 24 GHz. Comparable simulated results, i.e., gain values, are observed for $z < 0$. These far-field measurements were completed in an anechoic chamber and absorber was placed at the edges of the finite substrate to resemble an infinite slab. In addition, simulations assumed an infinite GDS for fair comparison.

2) Transmit Power Between Two SWLs: Measured insertion loss values are above 20 dB ($\geq$ 0.5 dB/mm) from 19.5 to 24.5 GHz as shown in Fig. 8(a). The realized test circuit utilized

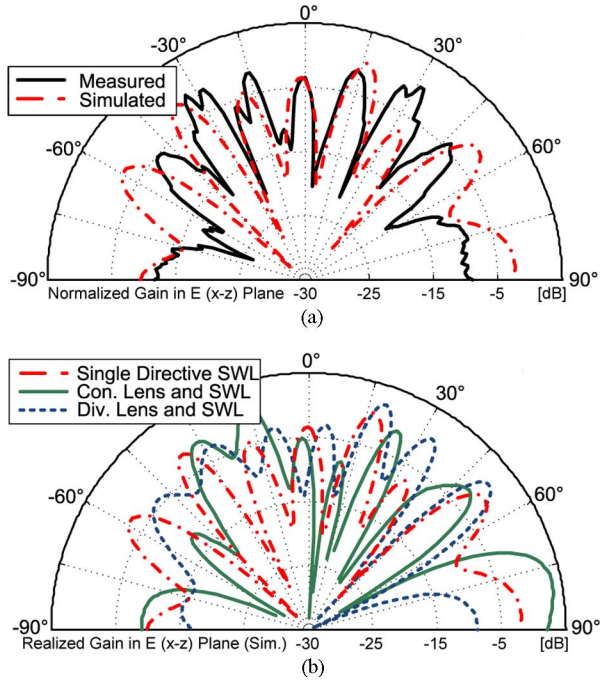

Fig. 7. Parasitic far-field radiation, $|E_\theta(\phi = 0^\circ)|$, from a single SWL (a) and with lenses (b). E plane referenced to main slot of the SWL.

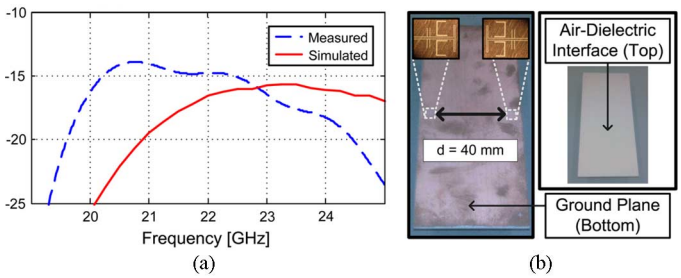

Fig. 8. Insertion loss, S_{21}, in dB (a) between 2 SWLs (b).

2 SWLs separated by $d = 40$ mm as shown in Fig. 8(b). Furthermore, these SWLs were placed a significant distance apart ($d \gg \lambda^{\mathrm{SW}}$) and consequently the circuit may be reasonable for a simple transmission analysis.

Thus these results suggest the utilized SWL sources can efficiently couple energy into the dominant SW mode of the slab providing bound and unidirectional guided-wave propagation.

III. Grating Lenses and System Applications

The diverging and converging metallic grating lenses were designed to achieve controlled SW propagation along a dielectric slab. Specifically, by the addition of these planar lenses, the excited TM SW field distributions can capacitively couple to the metallic strip segments, altering the phase velocity of the guided-wave, realizing refraction. The resultant field distribution on the GDS generated by the SW source and grating lenses are shown in Fig. 6(b) and (c).

A. Planar Grating Lens for SW Divergence

The divergence of TM SWs can be observed at 24 GHz in Fig. 6(b). For instance, the $|E_z|$ field distribution is $\geq$ 750 V/m in the 1840 mm^2 confined region (defined by $x \in [0, +40]$ mm

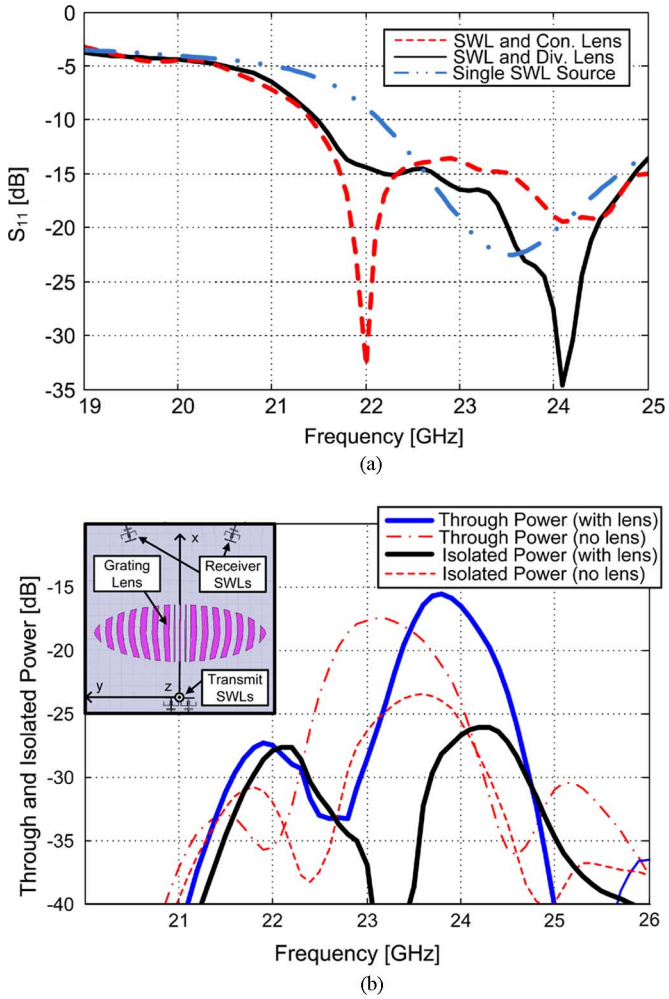

Fig. 9. (a) Simulated reflection loss values of the SW source and grating lenses. (b) Results of a novel 4-port hybrid coupler and increased performance using a grating lens. Through and isolated power defined as $|S_{31}|$ and $|S_{41}|$. Power is directed to the through port by a relative phase difference (of 60°) between transmit SWL sources.

and $y \in [-23, +23]$ mm). This suggests a 1.66 dB increase in area when compared to the single SWL source (when fixed x domains and field strength values are compared) thus suggesting increased spreading of TM SW power along the guiding surface. Moreover, field strength values increased by 9.5 dB at $x = 50$ mm and $y = \pm 25$ mm when compared to the single SW source. Reduced cross polarization levels are also observed ($|E_\phi(x, y = \pm 19\ \text{mm})| \leq 250$ V/m). In addition, the majority of the SW power is still bound and not parasitically radiated as shown in Fig. 7(b). Reflection loss values are also below 30 dB as shown in Fig. 9(a) at 24 GHz.

B. Planar Grating Lens for SW Convergence

In contrast, SWs converged towards the $\hat{x}$-axis for $x \in [10, 27]$ mm as shown in Fig. 6(c). In addition, $|E_z| \geq 750$ V/m in the 640 mm^2 confined region (defined by $x \in [0, +40]$ mm and $y \in [-8, +8]$ mm) suggesting a 7.51 dB decrease in area (for fixed domains and field strengths). The TM field distributions were reduced by 9.5 dB when compared to the single SWL source at $x = 40$ mm and $y = \pm 15$ mm. High cross polarizations levels are also shown at $x = +20$ mm and $y = \pm 10$ mm for the $|E_\phi|$ field strength plot ($|E_\phi(x, y = \pm 8\ \text{mm})| \leq 1250$ V/m). Improvements in the layout of the converging lens could minimize these high cross-polarization levels (or the TE SW excitation could be completely eliminated by the utilization of a single mode slab). Furthermore, the majority of the SW power is still bound and not radiated into the far-field as shown in Fig. 7(b) and reflection loss values are below 18 dB as shown in Fig. 9(a).

C. Guided-Wave Power Routing for Planar Circuit Systems

Using a two element array of SW sources a novel coupler can be realized. Essentially guided-waves are routed towards SWL receiver ports by changing the phase difference between transmit SWLs. Coupler performance can be improved by the addition of the diverging grating lens (since it offers best reflection loss values at the SWL design frequencies, 23–24 GHz). Specifically, if two transmit SWL sources are placed at the origin (ports 1 and 2) and receiver elements (ports 3 and 4) are placed at $28.1\angle \pm 17.6°$ mm as shown in the layout of the Fig. 9(b) inset, transmit [isolated] power can be increased [decreased] by at least 2.5 [15] dB. These results may be reasonable since similarities are observed in the measured and simulated values for the transmission test circuit (Fig. 8).

IV. Conclusion

Control of cylindrical SWs excited from a central SWL source have been investigated using planar metallic grating lenses. Surface-wave field distributions are provided at 23 GHz along with parasitic far-field radiation measurements. Metallic grating lenses were also developed for controlled SW propagation along the utilized GDS. Concepts are extended to a planar quasi-optical power coupler with isolations [directivities] ≤ -40 dB [≥ 24 dB] observed at 23.5 GHz.

References

[1] A. R. Perkons, Y. Qian, and T. Itoh, "TM surface wave power combining by planar active-lens amplifier," *IEEE Trans. Microw. Theory Tech.*, vol. 46, no. 8, pp. 775–783, 1998.

[2] H. Hammad, "A CPW-Based Slab Beam Quasi-Optical Power Combiner at Ka-Band," Ph.D. dissertation, Queen's Univ., Kingston, Ont., Canada, Mar. 2002.

[3] R. G. Rojas and K. W. Lee, "Surface wave control using nonperiodic parasitic strips in printed antennas," *Inst. Electr. Eng. Proc. Microw., Antennas Propag.*, vol. 148, no. 1, pp. 25–28, Feb. 2001.

[4] S. Mahmoud, Y. M. M. Antar, H. Hammad, and A. Freundorfer, "Theoretical considerations in the optimization of surface waves on a planar structure," *IEEE Trans. Antennas Propag.*, vol. 52, pp. 2057–2063, Apr. 2004.

[5] M. Ettorre, S. Bruni, G. Gerini, A. Neto, N. Llombart, and S. Maci, "Sector PCS-EBG antenna for low-cost high-directivity applications," *IEEE Antennas Wireless Propag. Lett.*, vol. 6, pp. 537–539, 2007.

[6] S. K. Podilchak, A. P. Freundorfer, and Y. M. M. Antar, "Surface-wave launchers for beam steering and application to planar leaky-wave antennas," *IEEE Trans. Antennas Propag.*, vol. 57, no. 2, pp. 355–363, Feb. 2009.

[7] R. E. Collin, *Foundations for Microwave Engineering*, 2nd ed. New York: Wiley-Intersci., 1992.

[8] E. Denlinger, "A frequency dependant solution for microstrip transmission lines," *IEEE Trans. Microw. Theory Tech.*, vol. 19, pp. 30–39, Jan. 1971.